Heliyon 10 (2024) e39549

Contents lists available at ScienceDirect

Heliyon

journal homepage: www.cell.com/heliyon

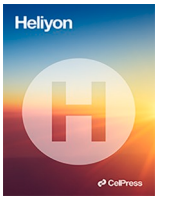

Research article

Hsa_circ_0004194 suppresses colorectal cancer progression via hsa-miR-27a-3p

Chen Lin [a,1], Hongjun Li [a,1], Huabin Gao [a,1], Shuai Zheng [a], Yu Wang [a], Yuting Wang [a], Yongyu Chen [a], Zhenwei Zhu [b], Pei Xia [a], Hujuan Shi [a,**], Anjia Han [a,*]

[a] *The Department of Pathology at the First Affiliated Hospital of Sun Yat-Sen University in Guangzhou, China*
[b] *The Oncology Department at Shenzhen Hospital of Southern Medical University in Shenzhen, China*

A R T I C L E I N F O

Keywords:
Colorectal cancer
hsa_circ_0004194
Hsa-miR-27a-3p
RXRα

A B S T R A C T

Aims: To investigate the functional role and the underlying molecular mechanisms associated with hsa_circ_0004194 in the context of colorectal cancer (CRC) and to elucidate its impact on cancer progression.

Results: A notable and statistically significant decrease in the expression levels of hsa_circ_0004194 was observed specifically within CRC tissues when compared to non-tumor colorectal mucosa tissues. Functional evaluations, such as CCK8 assays, plate clone formation analysis, and transwell migration assays, our study revealed hsa_circ_0004194 significantly reduced the activity behavior of CRC cells. This overexpression of hsa_circ_0004194 effectively hindered these key cellular processes, demonstrating its role in suppressing the aggressive behaviors of CRC cells. Additionally, in vivo experiments utilizing mouse xenograft models exhibited that the upregulation of hsa_circ_0004194 significantly attenuated tumor growth, reduced tumor volume, and diminished liver metastasis. Further mechanistic investigation, through the utilization of RNA pull-down and luciferase reporter assays, uncovered that hsa_circ_0004194 sequestered hsa-miR-27a-3p, thereby enhancing retinoic acid X receptor α (RXRα)' expression which is in CRC cells. Moreover, this circular RNA also impeded the signaling pathway of Wnt/β-catenin.

Conclusion: Our study is the first to demonstrate that hsa_circ_0004194 exhibits downregulated expression in CRC and functions as a ceRNA by binding to and sequestering hsa-miR-27a-3p, thereby modulating the RXRα/β-catenin signaling pathway to inhibit CRC progression. This discovery suggests that hsa_circ_0004194 holds significant potential as a therapeutic biomarker for patients with CRC.

* Corresponding author. The Pathology Department at The First Affiliated Hospital of Sun Yat-sen University, located at 58 Zhongshan Road II, Guangzhou, 510080, China.
** Corresponding author.
E-mail addresses: shihj@mail.sysu.edu.cn (H. Shi), hananjia@mail.sysu.edu.cn (A. Han).
[1] Lin Chen, Hongjun Li and Huabin Gao contributed equally to this work.

https://doi.org/10.1016/j.heliyon.2024.e39549
Received 28 July 2024; Received in revised form 4 October 2024; Accepted 16 October 2024
Available online 20 October 2024

1. Introduction

Globally, it is estimated that in 2022 the total number of CRC patients is about to pass the 2 million mark, with approximately 904,000 lives lost which attributed to this disease [1]. CRC ranks third in terms of incidence but second in mortality, highlighting the urgent need for novel and effective molecular targets. Despite advances in medical research, current treatment strategies for metastatic or recurrent CRC remain insufficient, highlighting the critical need for ongoing research and the development of new therapeutic approaches. Addressing these challenges will be crucial in improving patient outcomes and reducing the global burden of CRC.

Circular RNAs (circRNAs) constitute a distinct class of non-coding RNAs, recognized for their unique structural configuration. These molecules feature a loop that is closed by covalent bonds, which fundamentally sets them apart from other RNA types. Unlike conventional linear RNAs, circRNAs lack the 5′–3′ polarity and are devoid of a polyadenylated tail [2]. Growing research suggests that circRNAs play pivotal roles in colorectal cancer (CRC) progression through diverse mechanisms. For instance, hsa_circ_001680 modulates CRC proliferation and migration by sponging miR-340 [3]. circNEIL3 inhibits CRC tumor metastasis by interacting with the protein YBX1 [4]. circITGB6 enhances tumor metastasis by stabilizing PDPN mRNA [5]. Moreover, circ-YAP encodes a novel truncated protein containing 220 amino acids, facilitating CRC cancer metastasis [6].

miRNAs are short, noncoding RNA molecules that exert their effects by interacting with the 3′-untranslated regions (UTRs) of specific target genes. Through this interaction, they serve a vital function in silencing their expressions and regulating diverse cellular processes [7]. Our previous research revealed that CRC is substantially impacted by hsa-miR-27a-3p, which exerts a crucial influence throughout the development and advancement of this malignancy. This miRNAs achieves its effects by suppressing the expression of retinoic acid X receptor α (RXRα) and activating the β-catenin signaling pathway [8]. Recently, hsa-miR-27a-3p has been identified as a highly promising candidate for early intervention and treatment strategies in the early stages of CRC [9]. In early-stage CRC, genes such as AQP8, GUCA2B, and SPIB serve as important suppressor genes and are frequently co-expressed, with miR-27a-3p and miR-182-5p serving as potential mediators of these genes [10]. RXRα has been identified as a strong candidate driver that may be modulated by factors like cigarette smoking and body mass index (BMI) to influence CRC risk [11]. Furthermore, RXRα has been implicated in a novel CRC syndrome associated with a metabolic phenotype [12]. The process of activating the Wnt/β-catenin signaling pathway, a critical event in CRC development, has been observed in a significant majority of CRC patients [13].

In the course of our current research, we identified that hsa_circ_0004194 shows markedly lower expression levels in CRC tissue. Using bioinformatics analysis, we have pinpointed a possible interaction site between hsa_circ_0004194 and hsa-miR-27a-3p. These observations suggest a potential regulatory relationship between them. Nevertheless, the specific role and mechanism of hsa_circ_0004194 in CRC remain unclear. Therefore, our aim is to elucidate its function and how it is regulated during CRC progression.

2. Materials and methods

2.1. Cell lines and specimens

The human CRC cell lines SW480, SW620, HCT116, LOVO, SW1116, HT29, and mouse colon cancer cells MC38, along with the colonic epithelial cell line NCM460, were cultivated in various media, all sourced from Invitrogen. These cell lines, obtained from the Cell Bank of the Chinese Academy of Science and authenticated in 2015, were cultured in growth media enriched with 10 % fetal bovine serum and an antibiotic/antimycotic mixture. They were incubated at a temperature of 37 °C within an environment containing 5 % CO_2.

From January 2020 to December 2022, we collected fifty-two pairs of CRC tissues along with their corresponding non-tumor colorectal mucosal tissues from our institute. Each pair underwent a meticulous collection process. These samples were preserved in liquid nitrogen. Notably, none of the individuals in the study had received any form of radiotherapy or chemotherapy before their tumors were surgically removed. This research was granted approval by the Ethics Committee of the First Affiliated Hospital, Sun Yat-sen University.

2.2. Biotin labeled RNA pulldown assay

The biotinylated hsa_circ_0004194 probe (from RIBOBIO, China) was incubated with Streptavidin Magnetic Beads (Dynabeads™ Streptavidin Trial Kit, Thermofisher) for a duration of 2 h, maintained at room temperature. Subsequently, lysates from 2×10^7 SW480 cells were added and allowed to incubate with gentle rotation overnight at 4 °C. The subsequent step involved collecting the RNA compounds, which were then subjected to rigorous extraction procedures. And the RNA samples were subsequently subjected to analysis via reverse transcription-polymerase chain reaction (RT-PCR). This process was employed to obtain additional insights into the gene expression profiles.

2.3. Cell proliferation assay

1×10^3 cells were carefully plated into 96-well plates, with each well containing a medium that had been supplemented with a medium enriched with 10 % fetal bovine serum (FBS). Following the initial plating, the cells were allowed to incubate overnight under controlled conditions to facilitate adherence and initial growth. To monitor cell proliferation over time, we implemented the Cell Counting Kit-8 (CCK-8) assay as part of our experimental procedures, which was provided by Keygene (China). This assay involved measuring the optical density (OD) of the cells at 24 h intervals. Specifically, the OD values were obtained using a wavelength of 450

nm to accurately quantify the extent of cell proliferation.

2.4. Colony formation assay

This assay was conducted by seeding cells into 6-well plates. A density of 2×10^2 cells per well was used for this procedure, which were granted permission to proliferate for two weeks, followed by two thorough washes with PBS to remove any impurities. They were then fixed using 4 % paraformaldehyde to preserve their structure. The process of staining was carried out using a 0.5 % crystal violet solution. This procedure spanned a duration of 15 min, ensuring ample time for the stain to adequately penetrate and highlight the structures of interest. This methodical approach was crucial in enhancing the visibility of the samples under examination. The colony counts were established by first examining 10 randomly chosen microscopic fields. The average number of colonies observed across these fields was then calculated to determine the final count.

2.5. Transwell migration and Boyden invasion assays

Migration and invasion assays were conducted utilizing Transwell chambers equipped with 8 μm pore polycarbonate filters. For the assays, 1×10^5 cells in 100 μl of serum-free medium were added to the upper chambers, specifically maintained at a temperature of 37 °C, while being exposed to an atmosphere containing 5 % CO_2. This incubation process was meticulously sustained over a period of 18 h to ensure optimal environmental conditions for the experiment. Meanwhile, the lower chambers were filled with 500 μl of medium containingwith 10 % FBS. After removing cells from the top of the filters, the remaining ones were fixed with 4 % formaldehyde solution to fix them in place. Subsequently, these cells were stained using a 1 % crystal violet solution. Cell counts were averaged based on the number observed per view field.

2.6. Quantitative real-time PCR, Western blotting and immunohistochemical staining

Following our meticulously established protocols, as delineated in reference, we undertook a series of sophisticated experimental procedures to ensure robust and reliable results [14]. These methods mainly include quantitative PCR, etc. For a comprehensive understanding of our techniques, the specific primers employed for the qPCR assays are detailed, and the antibodies utilized in both Western blotting and IHC staining are exhaustively itemized. A comprehensive overview of these reagents is provided in Supplementary Tables 1–3 to ensure the accuracy and reproducibility of our results.

2.7. Animal experiments

Male Balb/c nude mice or C57 BL/6J mice, all aged 4–6 weeks, were procured from GemPharmatech (Nanjing, China). For the liver metastasis assay, the mice were first administered anesthesia to ensure they were properly sedated. Following this, a surgical procedure was conducted, involving the creation of a 1.0 cm incision on the upper left side of the abdomen. Utilizing tissue tweezers with precision, the spleen was meticulously removed from the abdominal cavity. Subsequent to the inoculation, 5×10^5 cells per mouse were introduced beneath the skin at the spleen of C57 BL/6J mice($n = 6$ per group). Following injection, pressure was applied to the needle site using a 75 % alcohol-soaked cotton ball for 2–3 min to arrest bleeding, and the incision was closed with sutures. After 3–4 weeks of intrasplenic injection, the mice were humanely euthanized. Subsequently, their livers were carefully extracted to facilitate the evaluation of the metastatic rate. For the xenograft assay, 1×10^7 cells per mouse were introduced beneath the skin at the left armpit of nude mice ($n = 6$ per group). Following the injection, tumor volumes were systematically measured every 3 days, continuing this monitoring routine over a period of approximately 30 days to track tumor growth and progression.

2.8. Luciferase reporter assay

To explore the interaction between hsa_circ_0004194 and hsa-miR-27a-3p, we synthesized both the wild-type and mutated 3′-UTR sequences of the former, cloned them into the psiCHECK2 vector, and co-transfected these constructs into HCT116 and SW480 cells along with mimics or a control mimic of the latter utilizing Lipofectamine 2000 (Invitrogen). Following a 48-h transfection period, the activities of both Firefly and Renilla luciferases were gauged utilizing the Dual Luciferase Reporter Assay Kit (Keygentec), to evaluate the interaction between the 3′-UTR sequence of hsa_circ_0004194 and Hsa-miR-27a-3p. This approach allowed us to assess the specific interactions between the two, providing valuable information for understanding the regulatory mechanisms involved. We validated the observed results by repeating the experiments and incorporating appropriate controls.

2.9. Statistical analyses

The data obtained from the cell culture experiments were subjected to analysis employing unpaired methods, two-tailed Student's t-tests to facilitate comparisons among the various experimental groups. The results of these comparisons were presented as mean ± SD. For the assessment involving the CCK8 assay, statistical evaluations were performed using univariate variance analysis, specifically a two-way ANOVA, to account for multiple factors affecting the results. The entire statistical analysis process was conducted with the assistance of SPSS version 24.0 and GraphPad Prism 6 software. To determine statistical significance, we adhered to a threshold wherein a P-value threshold below 0.05, which was considered indicative of a significant difference between the groups under study.

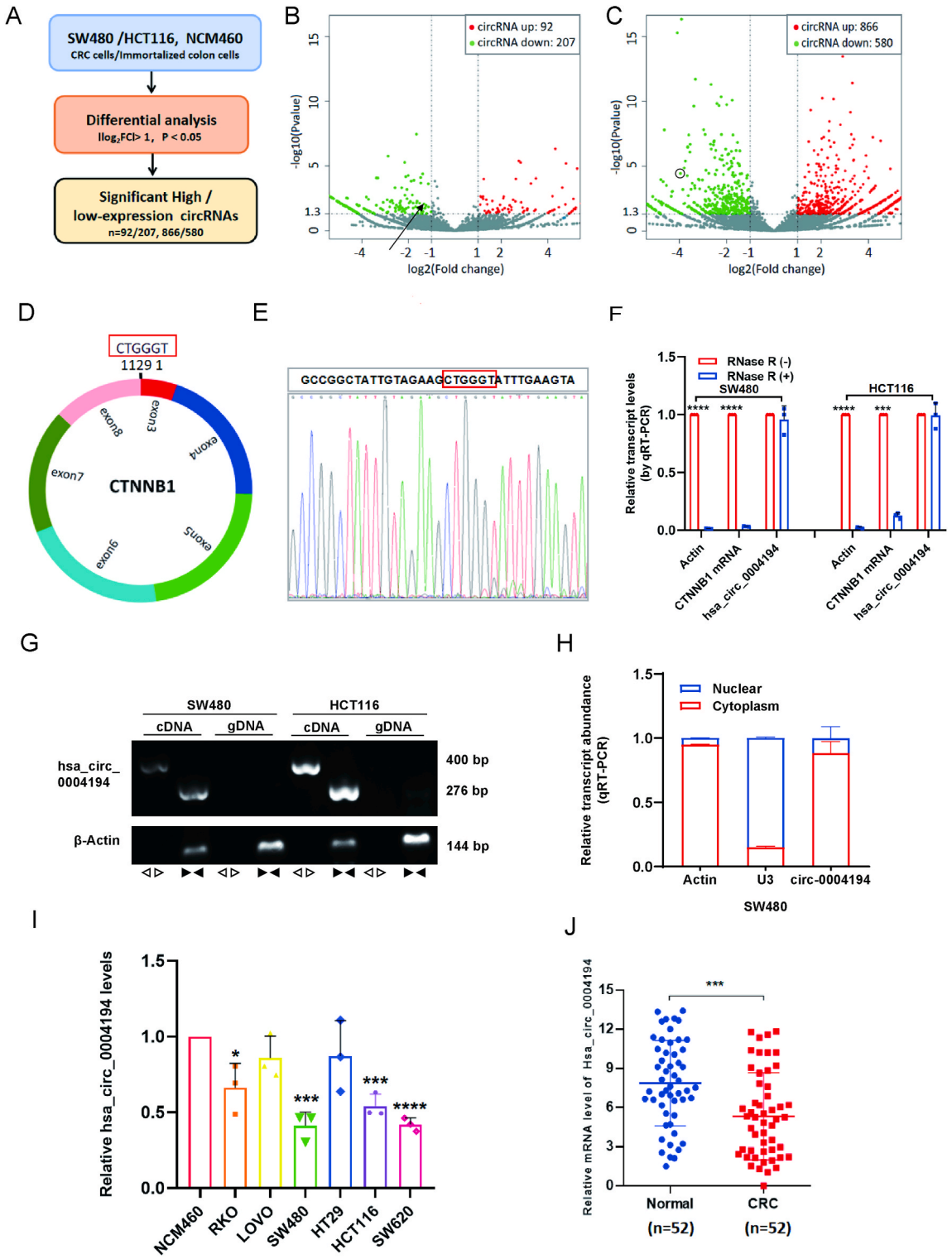

Fig. 1. Hsa_circ_0004194 expression in CRC.

(A) The design scheme of RNA-sequencing analyses. (B-C)Based on our analysis, we observed that SW480 cells (B) exhibited 92 circular RNAs with higher expression and 207 with lower expression compared with NCM460; HCT116 cells (C) displayed 866 circular RNAs with higher expression and 580 with lower expression compared with NCM460. (D) Schematic illustration showing the composition of hsa_circ_0004194. (E) The junction sequence was amplified by divergent primers and confirmed by sanger sequencing. (F) The transcript levels of CTNNB1 mRNA and hsa_circ_0004194 with or without RNase R digestion by real-time qRT-PCR. (G) Agarose gel electrophoresis (AGE) showed the PCR products which was amplified with

divergent or convergent primers using cDNA or gDNA as the template, respectively. actin as the internal reference. (H) RT-PCR analysis of hsa_circ_0004194 abundance in the cytoplasmic and nuclear fractions of SW480, while Actin and U3 as positive controls of cytoplasm and nuclear localization respectively. (I)hsa_circ_0004194 expression level in CRC cell lines and MCM460 cells by RT-PCR. (J) hsa_circ_0004194 expression levels in fresh CRC tissues (n = 52) and paired adjacent non-tumor colorectal mucosal tissues (n = 52) by RT-PCR. *p < 0.05, **p < 0.01, ***p < 0.001,****p < 0.0001.

Table 1
Hsa_circ_0004194 expression and its association. with clinicopathological features of CRC

Characteristics	No.	No. of low expression (%)	No.of high expression (%)	P value
Age (years)				0.577
<60	23	13(56.5 %)	10(43.5 %)	
≥60	29	13(44.8 %)	16(55.2 %)	
Gender				1
Male	33	16(48.5 %)	17(51.5 %)	
Female	19	10(52.6 %)	9 (47.4 %)	
Tumor size (cm)				0.393
<5	32	18(56.3 %)	14(43.7 %)	
≥5	20	8 (40.0 %)	12(60.0 %)	
Differentiation degree				0.508
Well	3	2 (66.7 %)	1(33.3 %)	
Moderate	45	23(51.1 %)	22(48.9 %)	
Poorly	4	1 (25.0 %)	3 (75.0 %)	
T stage				0.027
T0-T3	38	23(60.5 %)	15(39.5 %)	
T4	14	3 (21.4 %)	11(78.6 %)	
N stage				0.01
N0-N1	45	19(42.2 %)	26(57.8 %)	
N2	7	7(100.0 %)	0(0.0 %)	
M stage				0.116
M0	38	16(42.1 %)	22(57.9 %)	
M1	14	10(71.4 %)	4(28.6 %)	
TNM stage				0.264
I-II	23	9(39.1 %)	14(60.9 %)	
III–IV	29	17(58.6 %)	12(41.4 %)	

3. Results

3.1. Characterization and expression of hsa_circ_0004194 in CRC

To identify circRNAs in the progression of CRC, we performed RNA-sequencing analyses using two CRC cell lines (SW480 and HCT116) and the human normal colonic epithelial cell line NCM460 (Fig. 1A). Based on the sequencing data, we observed that SW480 cells exhibited 92 circular RNAs with high expression and 207 with low expression, when contrasted with NCM460 cells (Fig. 1B). Conversely, HCT116 cells displayed 866 circular RNAs with high expression and 580 with low expression (Fig. 1C). Intriguingly, we noted that hsa_circ_0004194 was under-expressed in both SW480 and HCT116 cells. To date, there were almost no reports on hsa_circ_0004194 in CRC.

By comparing the CircBase database, it has been found that hsa_circ_0004194 was composed of the reversed junction of exons 3–8 of the mature CTNNB1 mRNA from Chromosome 3, containing 1129 nucleotides(Fig. 1D). The head-to-tail junction sequence was verified by Sanger sequencing (Fig. 1E). We also characterized the resistance of hsa_circ_0004194 to endonucleases, validating the closed-loop structure and the high stability of hsa_circ_0004194. After RNase R digestion, the PCR product obtained from linear amplification decreased significantly, while there was no significant change in the circular form, verifying the resistance of hsa_circ_0004194 to RNA cleavage (Fig. 1F). We have further enhanced our understanding of the biological characteristics of hsa_circ_0004194. By designing convergent/divergent primers and utilizing PCR to amplify the genomic DNA and cDNA of colorectal cancer cell lines, electrophoresis analysis of the amplification products confirmed that hsa_circ_0004194 originated from the reverse splicing of mRNA, ruling out the possibility of genomic rearrangement or transposition (Fig. 1G). Additionally, through RNA nuclear-cytoplasmic fractionation and subsequent qRT-PCR analysis, we confirmed that hsa_circ_0004194 was specifically localized in the cytoplasm (Fig. 1H).

Our investigation into the expression of hsa_circ_0004194 in CRC cells (HCT116, SW480, LOVO, HT29, RKO, and SW620) and normal colorectal mucosal epithelial cell lines (NCM460) revealed a notably decreased expression in CRC cells, specifically SW480, SW620, HCT116, and RKO, compared to NCM460 cells (Fig. 1I). Additionally, hsa_circ_0004194 expression was assessed in a cohort consisting of 52 pairs of fresh CRC tissues and their corresponding non-tumor colorectal mucosal tissues. This assessment was carried out utilizing real-time PCR techniques. The results revealed a markedly lower expression of hsa_circ_0004194 in CRC tissues in contrast to the non-cancerous colorectal mucosal tissues (Fig. 1J). Furthermore, our analysis revealed a noteworthy relationship between hsa_circ_0004194 expression and both the T stage (P = 0.027) and N stage (P = 0.010) of CRC (Table 1).

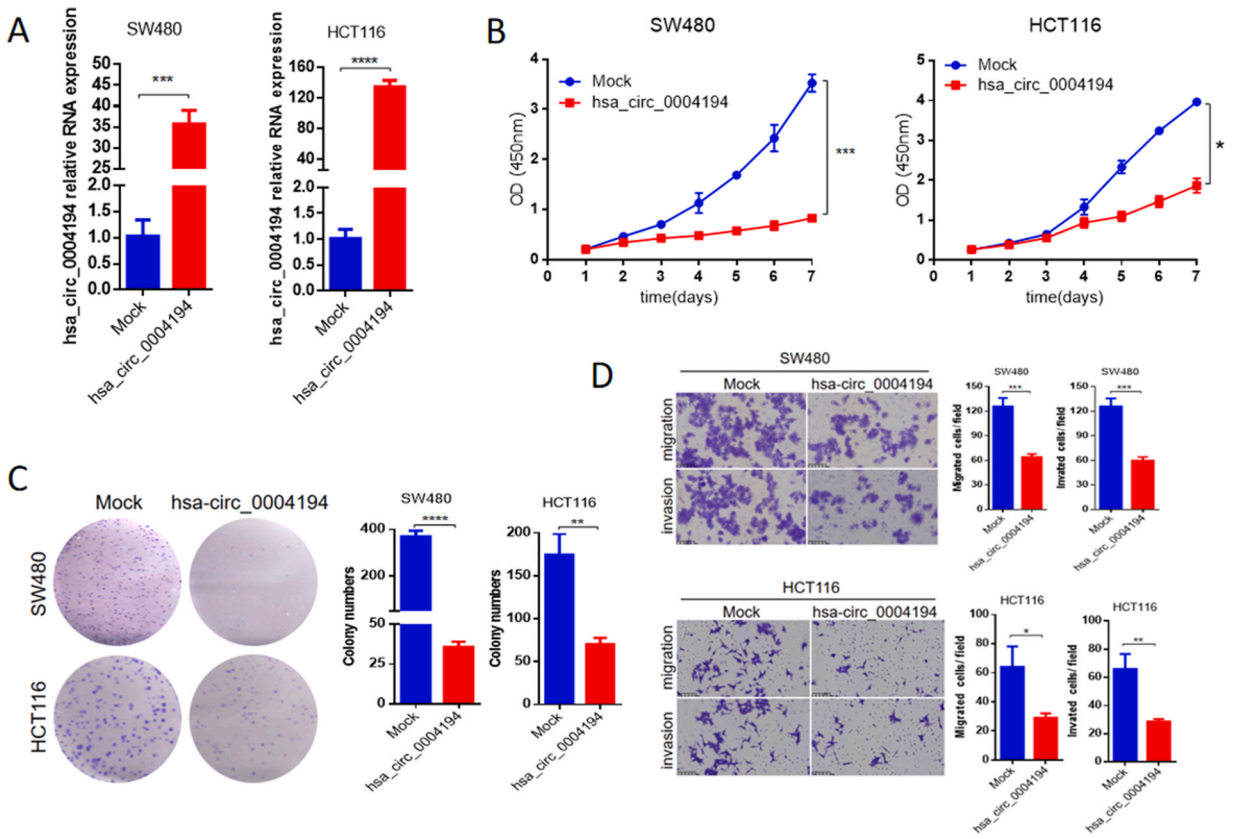

Fig. 2. Hsa_circ_0004194 suppresses the proliferation, migration and invasion of CRC cells.
(A) SW480 and HCT116 cells were infected with hsa_circ_0004194 or Mock lentivirus and Quantitative RT-PCR used to determine hsa_circ_0004194 expression. (B-C) hsa_circ_0004194 significantly suppressed cell proliferation (B) and colony formation (C) in SW480 and HCT116 cells by CCK-8 and colony formation assays assays, respectively.(D) Hsa_circ_0004194 significantly inhibited cell migration and invasion in SW480 and HCT116 cells. The scale bar in transwell assays indicated 100 μm. Data were all represented as mean ± SD (n = 3). *p < 0.05, **p < 0.01, ***p < 0.001.

3.2. *hsa_circ_0004194 inhibits CRC cell proliferation, migration, and invasion*

To initially delve into the cellular and biological functions of hsa_circ_0004194 in CRC, we established stable CRC cell lines overexpressing hsa_circ_0004194 in SW480 and HCT116 cells via lentiviral infection. The overexpression efficiency was subsequently confirmed through the application of qRT-PCR (Fig. 2A). CCK8 cell viability assays revealed that overexpressing hsa_circ_0004194 significantly impeded the proliferation of SW480 and HCT116 cells were in contrast to the control group (Fig. 2B). Furthermore, our analysis showed that overexpressing hsa_circ_0004194 greatly decreased the colony formation of SW480 and HCT116 cells were in contrast to the control group (Fig. 2C). Additionally, cell migration and invasion assays proved that overexpressing hsa_circ_0004194 markedly suppressed the migratory and invasive capabilities of SW480 and HCT116 cells were in contrast to the control group (Fig. 2D).

3.3. *hsa_circ_0004194 suppresses CRC growth and metastasis in mice*

In an effort to investigate the biological role of hsa_circ_0004194 in CRC within a living organism, we performed subcutaneous tumor formation experiments. This involved the injection of stable SW480 and HCT116 cells, which were engineered to overexpress hsa_circ_0004194, into Balb/c nude mice. Additionally, we injected hsa_circ_0004194-overexpressing stable MC38 cells into the spleens of C57BL/6J mice to study spleen-to-liver metastasis. Our subcutaneous tumor formation experiments in nude mice revealed that overexpressing hsa_circ_0004194 significantly reduced CRC tumor weight and volume was in contrast to the control group (Fig. 3A–C). IHC staining of tumor tissues extracted from the xenograft mice showed a notable decrease in Ki-67 expression in CRC tumors overexpressing hsa_circ_0004194 was in contrast to the control group (Fig. 3D). Furthermore, our spleen-to-liver metastasis experiments in C57BL/6J mice demonstrated that overexpressing hsa_circ_0004194 significantly suppressed CRC liver metastasis compared to the control group (Fig. 3E–G).

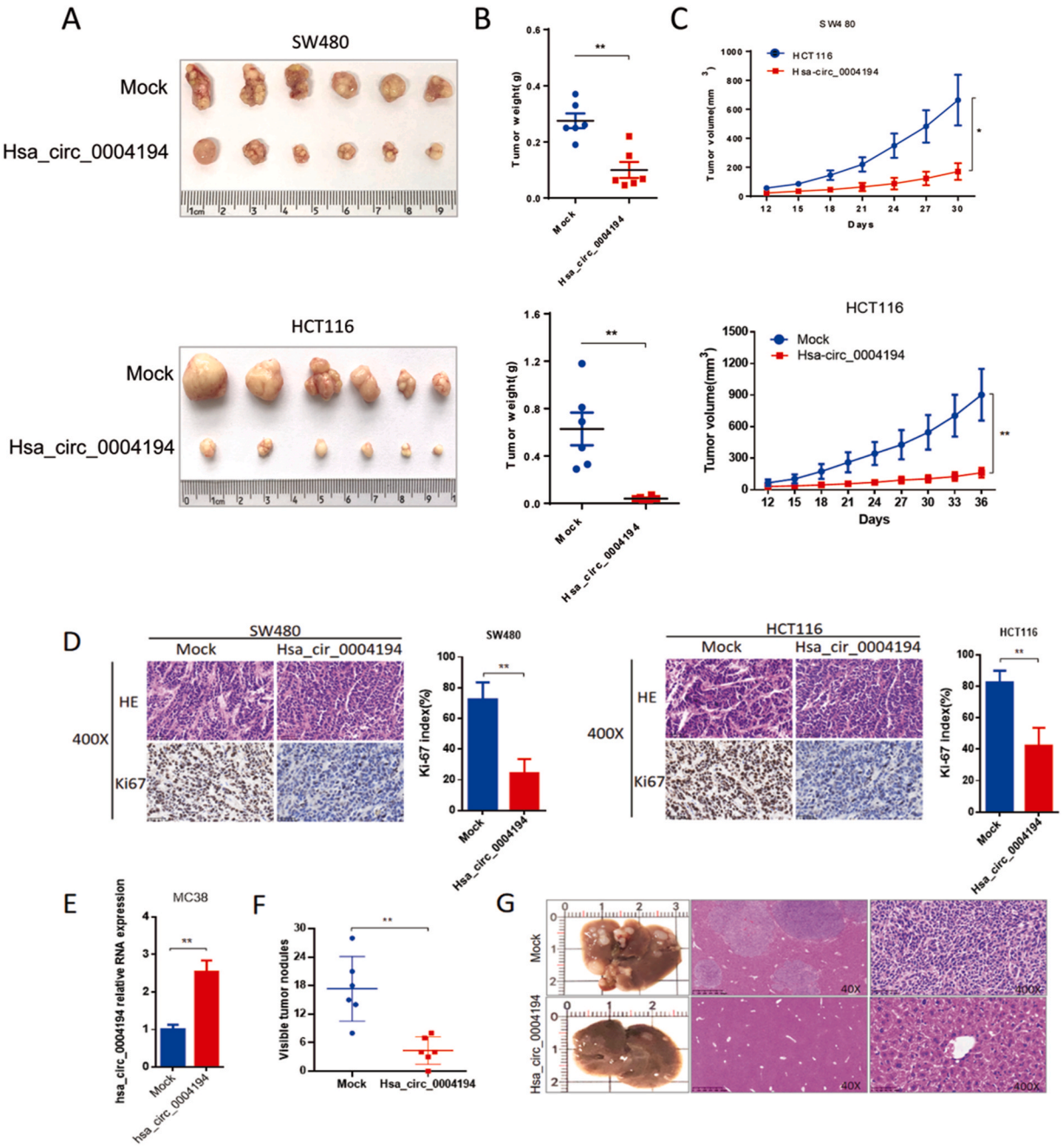

Fig. 3. Hsa_circ_0004194 suppresses the growth and metastasis of CRC in vivo.
(A–C) SW480 and HCT116 cells were injected subcutaneously into nude mice. After about a month, the tumors were dissected and photographed. Tumour volume was measured as length X width X height X 0.52. (D) H&E and IHC staining analyses were performed to demonstrate the morphology and detect Ki-67 expression in tumor tissues extracted from xenograft mice. (E) MC38 cells were infected with circ_0004194 or Mock lentivirus and Quantitative RT-PCR used to determine hsa_circ_0004194 expression. $5X10^5$ infected MC38 cells were injected into the spleen of C57 mice. Mice were then sacrificed and the liver tissues were sectioned and stained by H&E staining after about a month. (F) The number of visible metastases nodules was calculated. (G)Representative liver specimen and HE pictures. The scale bar in 40X and 400X photos indicated 625 μm and 50 μm. Data were represented as mean ± SD (n = 3). **p < 0.01. ***p < 0 0.001.

3.4. hsa_circ_0004194 serves the role of a sponge for hsa-miR-27a-3p in CRC

To investigate the potential role of hsa_circ_0004194 as a sponge regulating hsa-miR-27a-3p, we first test the hsa-miR-27a-3p expression in stably overexpressing hsa_circ_0004194 cell lines. The results showed that overexpression of hsa_circ_0004194 led to

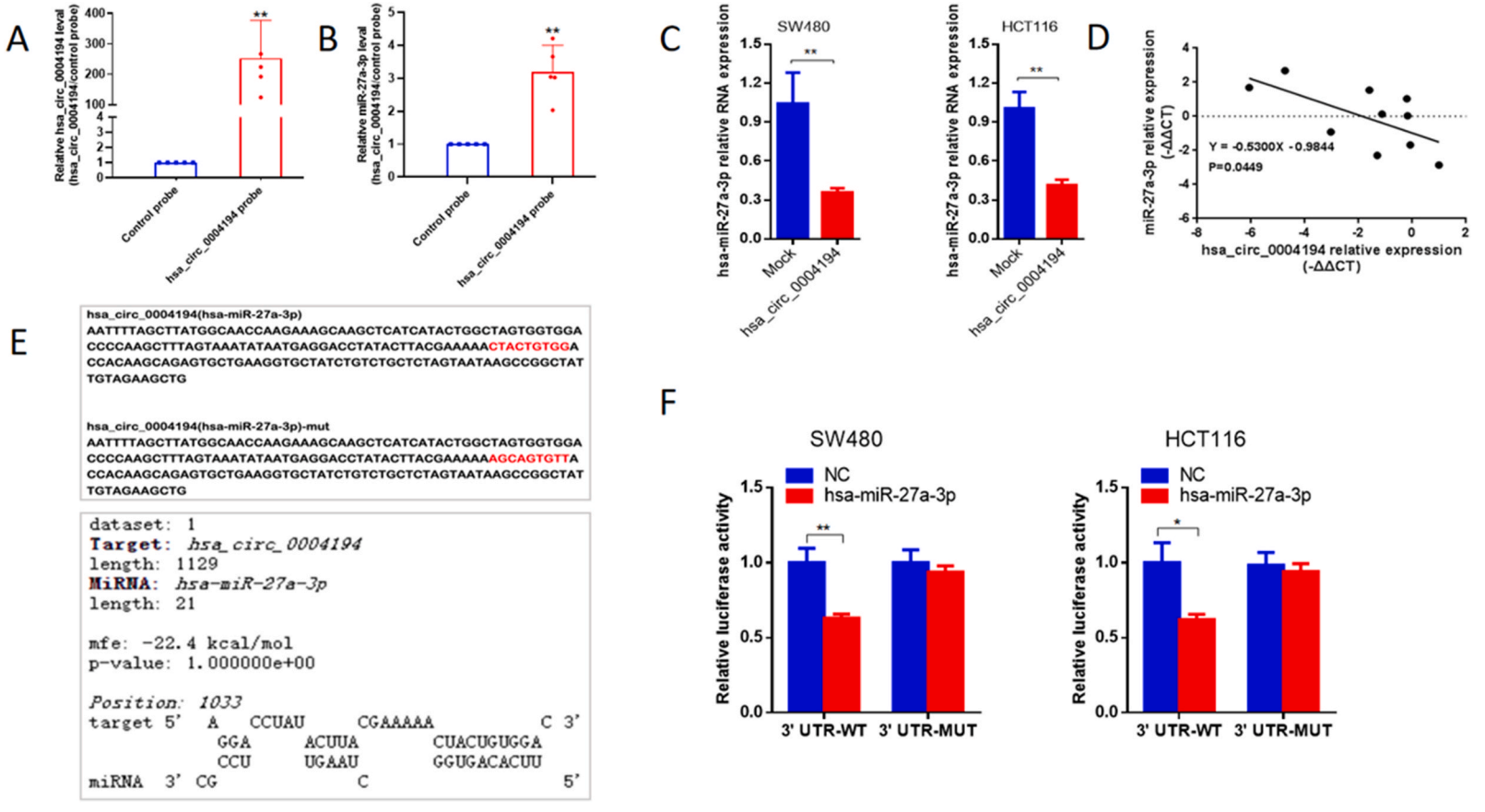

Fig. 4. Hsa_circ_0004194 directly binds to hsa-miR-27a-3p in CRC.
(A)hsa_circ_0004194 overexpression significantly down-regulated hsa-miR-27a-3p expression in SW480 and HCT116 cells.(B) Correlation analysis revealed that the expression of hsa_circ_0004194 and hsa-miR-27a-3p was negatively correlated in CRC tissues.(C-D)The expression levels of hsa_circ_0004194 and hsa-miR-27a-3p pulled down by biotin-labeled hsa_circ_0004194 probe and control probe in SW480 lysates. (E) The rnahybrid website predicted the possible binding targets of hsa_circ_0004194 and hsa-miR-27a-3p. (F)Dual luciferase assay confirmed that hsa-miR-27a-3p could bind specifically to hsa_circ_0004194 in SW480 and HCT116 cells. Data were all represented as mean ± SD (n = 3). *p < 0.05, **p < 0.01, ***p < 0.001.

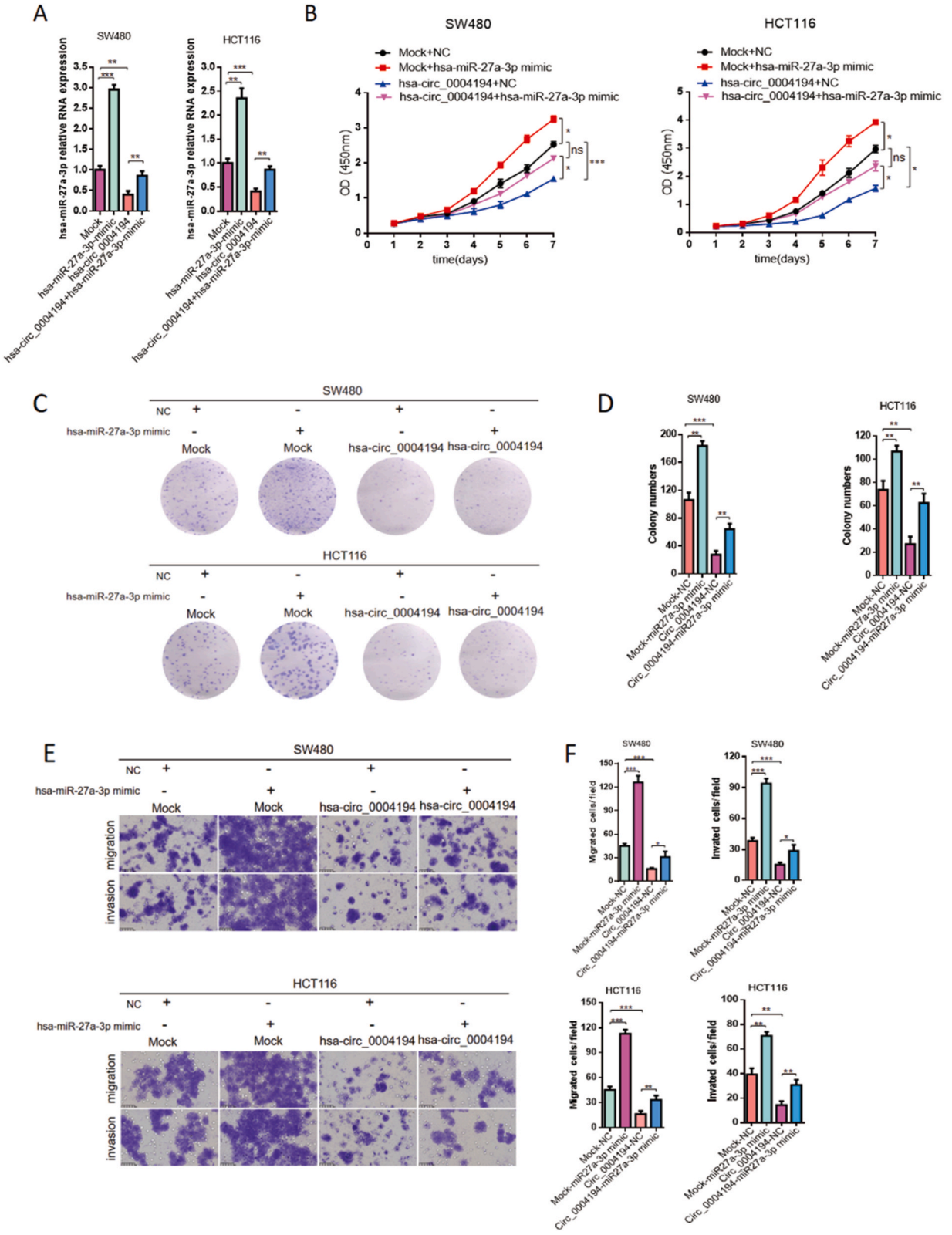

(caption on next page)

Fig. 5. Hsa_circ_0004194 suppresses CRC progression partially depending on hsa-miR-27a-3p.
(A) Overexpression efficiency of hsa-miR-27a-3p was detected by qRT-PCR. (B-E) hsa-miR-27a-3p could partially restore the inhibitory effect of hsa_circ_0004194 overexpression on the proliferation(B-C)、migration(D) and invasion(E)of CRC cells. The scale bar in transwell assays indicated 50 μm. Data were all represented as mean ± SD (n = 3). ns indicated no significance, *p < 0.05, **p < 0.01,***p < 0.001.

a notable downregulation of hsa-miR-27a-3p expression in SW480 and HCT116 cells in contrast to the control group (Fig. 4A). Correlation analysis revealed a negative correlation between the expressions of hsa_circ_0004194 and hsa-miR-27a-3p in CRC tissues (Fig. 4B). And then we conducted a detailed RNA pull-down assay. This assay employed a biotin-labeled probe specifically designed to target the back-splice junction sequences of hsa_circ_0004194. Our findings indicated that hsa-miR-27a-3p was significantly enriched by hsa_circ_0004194 (Fig. 4C–D). Subsequently, we predicted potential binding sites between hsa_circ_0004194 and hsa-miR-27a-3p using the rnahybrid website and conducted mutagenesis experiments (Fig. 4E). Finally, dual-luciferase reporter assays confirmed the specific binding between hsa-miR-27a-3p and hsa_circ_0004194 in SW480 and HCT116 cells (Fig. 4F).

3.5. *hsa_circ_0004194 inhibits CRC progression through hsa-miR-27a-3p*

To delve deeper into the mechanisms underlying hsa_circ_0004194's regulation of CRC progression, we investigated whether it modulated RXRα and impeded the β-catenin signaling pathway via hsa-miR-27a-3p. To functionally validate this, we transiently overexpressed hsa-miR-27a-3p in SW480 and HCT116 cell lines that stably overexpressed hsa_circ_0004194. The transfection efficiency was confirmed using qRT-PCR (Fig. 5A). Our CCK8 cell viability and colony formation assays revealed that the overexpression of hsa-miR-27a-3p partially counteracted the inhibitory effects of hsa_circ_0004194 overexpression on the proliferation and colony formation abilities of SW480 and HCT116 cells, in comparison to the control group (Fig. 5B–D).Furthermore, assessments from cell migration and invasion assays illustrated that overexpressing hsa-miR-27a-3p partly reinstated the migratory and invasive capacities of SW480 and HCT116 cells, which had been suppressed by hsa_circ_0004194 overexpression (Fig. 5E–F).

3.6. *Hsa_circ_0004194/hsa-miR-27a-3p/RXRα/β-catenin signaling pathway takes part in CRC progression*

Our findings revealed an elevation in the mRNA and protein expression levels of RXRα in SW480 and HCT116 cells with hsa_circ_0004194 overexpression, was in contrast to the control group (Fig. 6A–B). Analogously, the research identified a reduction in the mRNA and protein expression levels of β-catenin, cyclinD1, and c-Myc in SW480 and HCT116 cells following hsa_circ_0004194 overexpression, relative to the control group (Fig. 6C–D). Additionally, the augmentation of hsa-miR-27a-3p was found to partially mitigate the impact of hsa_circ_0004194 overexpression on the mRNA and protein expression levels of β-catenin, cyclinD1, and c-Myc in SW480 and HCT116 cells, as compared to the control group (Fig. 6E).

4. Discussion

CircRNAs, a recently discovered non-coding RNAs (ncRNAs), are prevalent across numerous species [15]. Notably, they occupy a pivotal position in regulating gene transcription and expression, thereby highlighting their crucial role in a broad spectrum of biological and pathological processes [16]. circRNAs have differential expression patterns and are involved in CRC tumor growth and progression [17,18]. Our study has uncovered significant alterations in hsa_circ_0004194 expression, which notably exhibited a correlation with the tumor's T stage and lymph node metastasis in CRC patients. Furthermore, overexpressing hsa_circ_0004194 significantly impeded cell proliferation and migration, and it was corroborated by xenograft model results. Collectively, these observations imply that hsa_circ_0004194 operates as a gene responsible for tumor suppression, significantly influencing the progression of CRC. Typically, the functionality of one gene is explored through methods of overexpression or knockdown; however, since hsa_circ_0004194 exhibits underexpression in prevalent colorectal cancer cell lines, we employ gene overexpression as our approach to investigate its role.

The involvement of the miRNA member, hsa-miR-27a-3p, in the oncogenic mechanisms underlying colorectal cancer has been documented in several studies [19,20]. Our previous research revealed that miR-27a-3p specifically targets RXRα. This interaction, in turn, facilitates the progression of CRC by triggering the activation of the Wnt/β-catenin signaling pathway, which is known to drive tumor growth and metastasis. Given that circRNAs are often viewed as miRNA sponges, they have the potential to reverse the inhibitory effects of miRNAs [21]. In this study, our findings indicated that hsa_circ_0004194 functions as a competing endogenous RNA (ceRNA) to administer the downstream targets of Hsa-miR-27a-3p. This finding underscores the intricate regulatory network involving circRNAs and miRNAs in colorectal cancer.

RXRα is a protein-coding gene belonging to the superfamily of transcriptional regulators that includes steroid and thyroid hormone receptors. In recent years, RXRα has garnered attention for its role in tumor development. It contributes to myeloid maturation in both mice and humans, and the deletion of RXRα and RXRβ enhances leukemic growth in mice [22]. In bladder cancer, mutations in RXRα lead to urothelial cell proliferation by activating peroxisome proliferator-activated receptors. In triple-negative breast cancer, RXRα works with the EGR1 transcription factor to regulate CCL2 expression via the TGF-β pathway. In prostate cancer, RXRα interacts with miR-191 to enhance resistance to radiation. Furthermore, modulating RXRα can make chronic myeloid leukemia cells more responsive to imatinib therapy. Additionally, RXRα is directly targeted by miR-27a-3p, influencing its oncogenic effects in colorectal cancer [23–25]. Overall, RXRα is a crucial and versatile player in cancer development and therapy. Through this research, it was revealed that

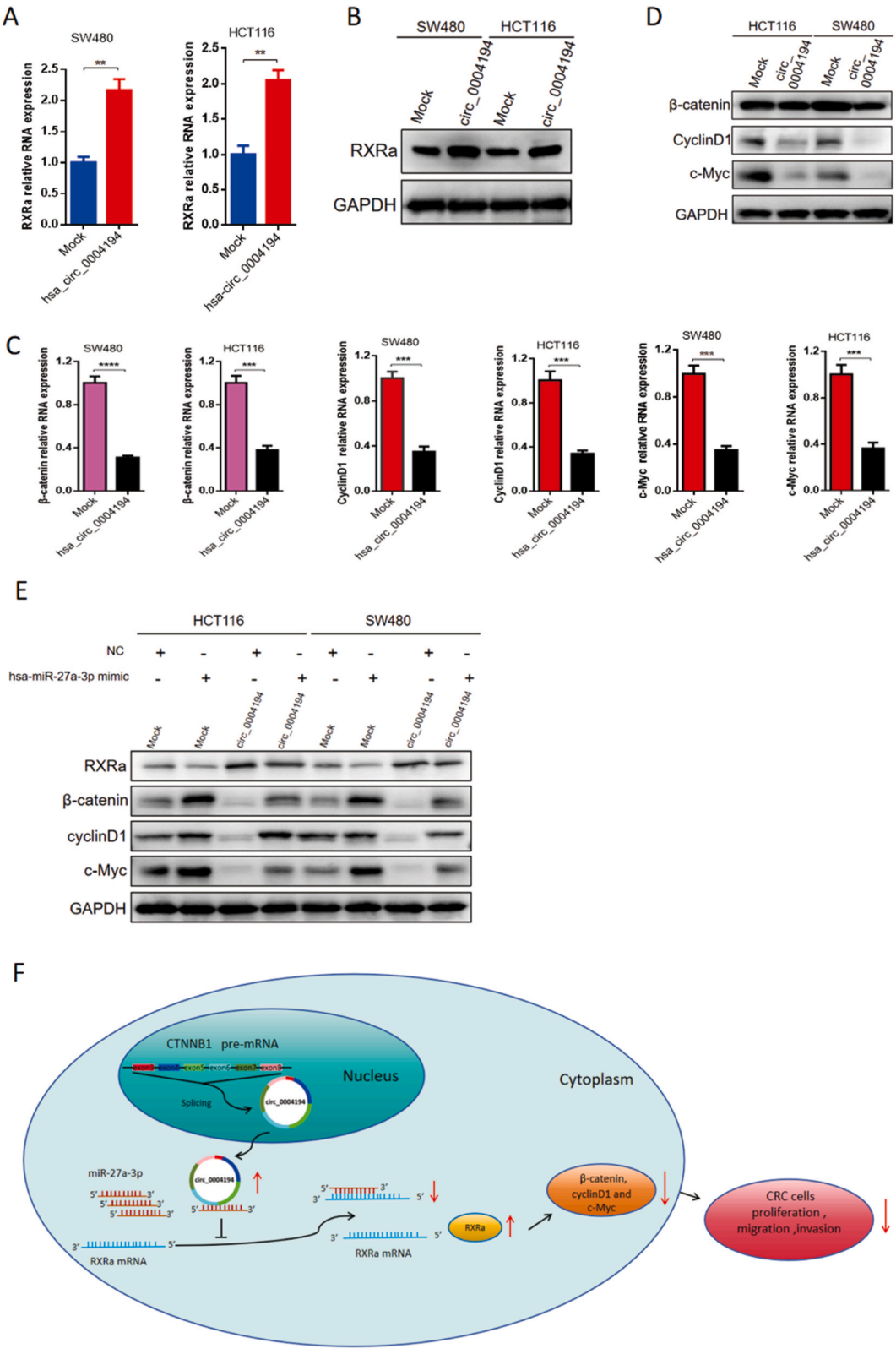

(caption on next page)

Fig. 6. Hsa_circ_0004194/miR-27a-3p/RXRα/β-catenin signaling pathway involved in CRC progression.
(A) The mRNA and (B) protein expression levels of RXRα were up-regulated after overexpression of Circ_0004194 in SW480 and HCT116. (C-D)The mRNA (C) and protein (D) expression levels of β-catenin, cyclinD1 and c-Myc were down-regulated in SW480 and HCT116 with overexpression of hsa_circ_0004194. (E)hsa-miR-27a-3p could partially restore the effects of Hsa_circ_0004194 overexpression on protein expression levels of RXRα, β-catenin, cyclinD1 and c-Myc in SW480 and HCT116 cells. (F) The schematic illustration showing the underlying mechanism of hsa_circ_0004194 in the progression of CRC.

overexpression of hsa_circ_0004194 upregulates RXRα expression. Notably, the changes in RXRα expression induced by hsa_circ_0004194 overexpression could be reversed by the hsa-miR-27a-3p mimic.

The loss or inactivation of adenomatous polyposis coli (APC) triggers the continuous activation of the Wnt/β-catenin signaling pathway, which is widely considered a crucial initiating factor in the progression of CRC. This pathway's activation is observed in a significant majority of CRC patients [13]. The impact of this signaling cascade is significant, as it plays a critical role in both the initiation and advancement of the disease. Within this pathway, key components such as β-catenin, cyclinD1, and c-Myc are frequently deregulated in this malignancy. This study reveals that the overexpression of hsa_circ_0004194 leads to the downregulation of these key proteins, suggesting that this circular RNA may intervene in the signaling cascade, ultimately contributing to a reduction in cell proliferation and tumorigenesis.

In summary, our study is the first to reveal that hsa_circ_0004194 exhibits downregulated expression in CRC. This circular RNA acts as a ceRNA by binding to and sequestering hsa-miR-27a-3p. Through this interaction, the regulation of RXRα expression is modulated. This modulation, in turn, significantly impacts the activation of the Wnt/β-catenin signaling pathway, thereby influencing the progression of CRC. As a consequence, this modulation significantly influences the activation of the Wnt/β-catenin signaling pathway. The pathway, in turn, plays a crucial role in tumor progression and metastasis. Our findings not only advance the understanding of circRNA functions in CRC but also highlight potential therapeutic targets for disrupting this regulatory network. This insight opens avenues for further research into targeted therapies to combat CRC more effectively.

CRediT authorship contribution statement

Chen Lin: Writing – original draft, Visualization, Funding acquisition, Data curation. **Hongjun Li:** Visualization, Validation. **Huabin Gao:** Validation, Data curation. **Shuai Zheng:** Validation, Investigation. **Yu Wang:** Data curation. **Yuting Wang:** Validation. **Yongyu Chen:** Methodology, Investigation. **Zhenwei Zhu:** Formal analysis, Data curation. **Pei Xia:** Software, Resources. **Hujuan Shi:** Supervision, Project administration. **Anjia Han:** Writing – review & editing, Supervision, Project administration, Funding acquisition.

Ethics statement

This research was granted approval by IEC for Clinical Research and Animal Trials of the First Affiliated Hospital of Sun Yat-sen university.Waiver/exempt was granted by the First Affiliated Hospital, Sun Yat-sen University Ethics Committee for this purpose. The Approval No. is IEC[2024]154.

Declaration of competing interest

The authors declare that they have no known competing financial interests or personal relationships that could have appeared to influence the work reported in this paper.

Acknowledgment

The present research is financially supported by grants from the Natural Science Foundation of Guangdong province, specifically grant numbers 2021A15-15012379 and 2022A15-15012550 and the National Natural Science Foundation of China (NO. 82103504).

Appendix A. Supplementary data

Supplementary data to this article can be found online at https://doi.org/10.1016/j.heliyon.2024.e39549.

References

[1] F. Bray, M. Laversanne, H. Sung, J. Ferlay, R.L. Siegel, I. Soerjomataram, A. Jemal, Global cancer statistics 2022: GLOBOCAN estimates of incidence and mortality worldwide for 36 cancers in 185 countries, CA Cancer J Clin 74 (3) (2024 May-Jun) 229–263.
[2] X. Chen, M. Zhou, L. Yant, C. Huang, Circular RNA in disease: basic properties and biomedical relevance, Wiley Interdiscip Rev RNA 13 (6) (2022 Nov) e1723.
[3] X. Jian, H. He, J. Zhu, Q. Zhang, Z. Zheng, X. Liang, L. Chen, M. Yang, K. Peng, Z. Zhang, T. Liu, Y. Ye, H. Jiao, S. Wang, W. Zhou, Y. Ding, T. Li, Hsa_circ_001680 affects the proliferation and migration of CRC and mediates its chemoresistance by regulating BMI1 through miR-340, Mol. Cancer 19 (1) (2020 Jan 31) 20.

[4] S. Chen, K. Li, J. Guo, H.N. Chen, Y. Ming, Y. Jin, F. Xu, T. Zhang, Y. Yang, Z. Ye, W. Liu, H. Ma, J. Cheng, J.K. Zhou, Z. Li, S. Shen, L. Dai, Z.G. Zhou, H. Xu, Y. Peng, circNEIL3 inhibits tumor metastasis through recruiting the E3 ubiquitin ligase Nedd4L to degrade YBX1, Proc Natl Acad Sci U S A 120 (13) (2023 Mar 28) e2215132120.
[5] K. Li, J. Guo, Y. Ming, S. Chen, T. Zhang, H. Ma, X. Fu, J. Wang, W. Liu, Y. Peng, A circular RNA activated by TGFβ promotes tumor metastasis through enhancing IGF2BP3-mediated PDPN mRNA stability, Nat. Commun. 14 (1) (2023 Oct 28) 6876.
[6] K. Zeng, J. Peng, Y. Xing, L. Zhang, P. Zeng, W. Li, W. Zhang, Z. Pan, C. Zhou, J. Lin, A positive feedback circuit driven by m6A-modified circular RNA facilitates colorectal cancer liver metastasis, Mol. Cancer 22 (1) (2023 Dec 13) 202.
[7] C. Occhipinti, R. La Russa, N. Iacoponi, J. Lazzari, A. Costantino, N. Di Fazio, F. Del Duca, A. Maiese, V. Fineschi, miRNAs and substances abuse: clinical and forensic pathological implications: a systematic review, Int. J. Mol. Sci. 24 (23) (2023 Dec 4) 17122.
[8] J. Liang, J. Tang, H. Shi, H. Li, T. Zhen, J. Duan, L. Kang, F. Zhang, Y. Dong, A. Han, miR-27a-3p targeting RXRα promotes colorectal cancer progression by activating Wnt/β-catenin pathway, Oncotarget 8 (47) (2017 Jul 26) 82991–83008.
[9] J.C. Huang, M.C. Li, I.C. Huang, J.M. Hu, W.Z. Lin, Y.T. Chang, Gene Co-expression and miRNA regulation: a path to early intervention in colorectal cancer, Hum. Gene Ther. 35 (19–20) (2024) 855–867. Oct.
[10] J.M. Hu, P.Y. Liu, Y.C. Chen, W.Z. Lin, Y.C. Chou, W.C. Tsai, C.M. Chu, C.C. Wu, Y.T. Chang, A co-regulatory network of SPIB, AQP8, and GUCA2B related to immune infiltration for early-stage colorectal cancer in silico and in vitro, Am. J. Cancer Res. 13 (11) (2023 Nov 15) 5271–5288.
[11] M. Devall, S. Eaton, C. Yoshida, S.M. Powell, G. Casey, L. Li, Assessment of colorectal cancer risk factors through the application of network-based approaches in a racially diverse cohort of colon organoid stem cells, Cancers 15 (14) (2023 Jul 9) 3550.
[12] K.K. Lam, R. Sethi, G. Tan, S. Tomar, M. Lo, C. Loi, C.L. Tang, E. Tan, P.S. Lai, P.Y. Cheah, The orphan nuclear receptor NR0B2 could be a novel susceptibility locus associated with microsatellite-stable, APC mutation-negative early-onset colorectal carcinomas with metabolic manifestation, Genes Chromosomes Cancer 60 (2) (2021 Feb) 61–72.
[13] J. Bian, M. Dannappel, C. Wan, R. Firestein, Transcriptional regulation of Wnt/β -catenin pathway in colorectal cancer, Cells 9 (9) (2020) 2125.
[14] Y. Yang, Y. Ma, H. Gao, T. Peng, H. Shi, Y. Tang, H. Li, L. Chen, K. Hu, A. Han, A novel HDGF-ALCAM axis promotes the metastasis of Ewing sarcoma via regulating the GTPases signaling pathway, Oncogene 40 (4) (2021 Jan) 731–745.
[15] X.Y. Feng, S.X. Zhu, K.J. Pu, H.J. Huang, Y.Q. Chen, W.T. Wang, New insight into circRNAs: characterization, strategies, and biomedical applications, Exp. Hematol. Oncol. 12 (1) (2023 Oct 12) 91.
[16] K. Nemeth, R. Bayraktar, M. Ferracin, G.A. Calin, Non-coding RNAs in disease: from mechanisms to therapeutics, Nat. Rev. Genet. 25 (3) (2024 Mar) 211–232.
[17] J. Mao, Y. Lu, Roles of circRNAs in the progression of colorectal cancer: novel strategies for detection and therapy, Cancer Gene Ther. 31 (6) (2024 Jun) 831–841.
[18] A. Khalafizadeh, S.D. Hashemizadegan, F. Shokri, B. Bakhshinejad, K. Jabbari, M. Motavaf, S. Babashah, Competitive endogenous RNA networks: decoding the role of long non-coding RNAs and circular RNAs in colorectal cancer chemoresistance, J. Cell Mol. Med. 28 (7) (2024 Apr) e18197.
[19] C. Su, D.P. Huang, J.W. Liu, W.Y. Liu, Y.O. Cao, miR-27a-3p regulates proliferation and apoptosis of colon cancer cells by potentially targeting BTG1, Oncol. Lett. 18 (3) (2019 Sep) 2825–2834.
[20] W. Liu, Z. Zhang, X. Luo, K. Qian, B. Huang, J. Deng, C. Yang, M6A promotes colorectal cancer progression via regulating the miR-27a-3p/BTG2 pathway, J Oncol 2023 (2023 Feb 10) 7097909.
[21] S. Chen, L. Ji, Y. Wang, L. Zhang, M. Xu, Y. Su, X. Zhang, lncRNA RMST suppresses the progression of colorectal cancer by competitively binding to miR-27a-3p/RXRα axis and inactivating Wnt signaling pathway, Acta Biochim. Biophys. Sin. 55 (5) (2023 May 29) 726–735.
[22] O. Di Martino, M.A. Ferris, G. Hadwiger, S. Sarkar, A. Vu, M.P. Menéndez-Gutiérrez, M. Ricote, J.S. Welch, RXRA DT448/9PP generates a dominant active variant capable of inducing maturation in acute myeloid leukemia cells, Haematologica 107 (2) (2022 Feb 1) 417–426.
[23] A.M. Halstead, C.D. Kapadia, J. Bolzenius, C.E. Chu, A. Schriefer, L.D. Wartman, G.R. Bowman, V.K. Arora, Bladder-cancer-associated mutations in RXRA activate peroxisome proliferator-activated receptors to drive urothelial proliferation, Elife 6 (2017 Nov 16) e30862.
[24] A.M. Gorbacheva, A.N. Uvarova, A.S. Ustiugova, A. Bhattacharyya, K.V. Korneev, D.V. Kuprash, N.A. Mitkin, EGR1 and RXRA transcription factors link TGF-β pathway and CCL2 expression in triple negative breast cancer cells, Sci. Rep. 11 (1) (2021 Jul 8) 14120.
[25] J. Ray, C. Haughey, C. Hoey, J. Jeon, R. Murphy, L. Dura-Perez, N. McCabe, M. Downes, S. Jain, P.C. Boutros, I.G. Mills, S.K. Liu, miR-191 promotes radiation resistance of prostate cancer through interaction with RXRA, Cancer Lett. 473 (2020 Mar 31) 107–117.